

# Supporting Information: Designing Two- Dimensional Temperature Profiles Using Tunable Thermoplasmonics

*Sergey S. Kharintsev<sup>1\*</sup>, Anton V. Kharitonov<sup>1</sup>, Elena A. Chernykh<sup>1</sup>, Alexander M. Alekseev<sup>1</sup>,  
Nikolai A. Filippov and Sergei G. Kazarian<sup>3</sup>*

<sup>1</sup>Department of Optics and Nanophotonics, Institute of Physics, Kazan Federal University,  
Kremlevskaya, 16, Kazan, 420008, Russia

<sup>2</sup>National Research University “MIET”, Moscow, Moscow, 124498, Russia

<sup>3</sup>Department of Chemical Engineering, Imperial College London, SW7 2AZ, United Kingdom

\*To whom correspondence should be addressed. E-mail: (S.S.K.) [skharint@gmail.com](mailto:skharint@gmail.com)

## **A calibration plot based on the temperature-dependent Raman shift**

Due to thermal (Boltzmann) pumping of excited vibrational levels, the lattice spacing and the lifetime of optical phonons are sensitive to temperature. This allows us to introduce intensity-, shift- and linewidth-based probes, respectively. The intensity (anti-Stokes/Stokes ratio) based probe features the most sensitive performance. However, this approach suffers from non-Boltzmann heating known as vibrational pumping.<sup>1,2</sup> This effect basically impacts resonant nanostructures. In the regime of vibrational pumping, the anti-Stokes/Stokes ratio

exhibits a linear dependence of the pump power for different Si pillar heights, as shown in Fig. S1, and, as a result, this leads to overestimating the temperature. The linewidth-based probe is less sensitive to temperature compared to the others, but this provides more robust results for materials under stress. Here, we will utilize the shift-based probe. For most materials, the specific Stokes peaks are red-shifted with increasing temperature. The Stokes peak shift  $\Delta(T)$  as a function of  $T$  is determined as follows<sup>3,4</sup>

$$\Delta(T) = \Omega(T) - \Omega(T_0) = A \left( 1 + \frac{2}{e^{\frac{h\omega_0}{2kT}} - 1} \right) + B \left( 1 + \frac{3}{e^{\frac{h\omega_0}{3kT}} - 1} + \frac{3}{(e^{\frac{h\omega_0}{3kT}} - 1)^2} \right) \quad (\text{S1})$$

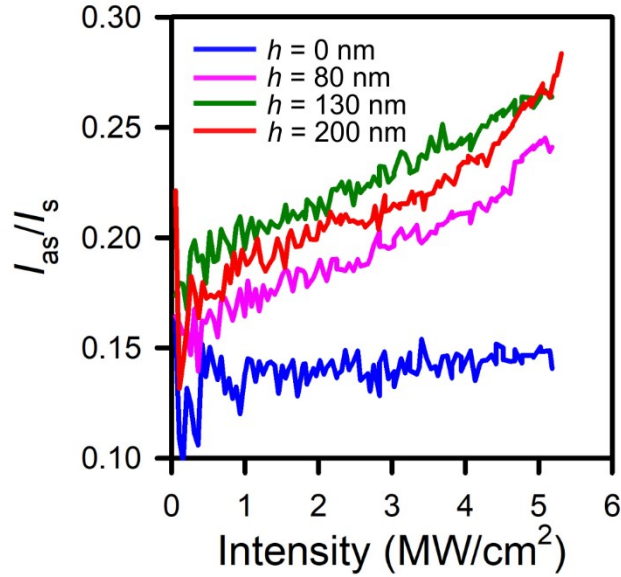


**Figure S1.** Dependence of an anti-Stokes and Stokes intensities ratio vs the pumping intensity for different Si pillar heights.

where  $A$  and  $B$  are constants specific to materials,  $\omega_0$  is the incident photon frequency,  $\Omega$  is a phonon frequency,  $h$  is the Plank's constant,  $k_B$  is the Boltzmann's coefficient,  $T$  is the absolute temperature of a sample in unit of  $K$ ,  $T_0$  is equal to 0 K. For silicon, we found the

following values  $A = -4.391 \text{ cm}^{-1}$  and  $B = -0.042 \text{ cm}^{-1}$  using temperature-dependent Raman measurements in the range from 25°C to 600°C (see Fig. S2). As seen from the figure, the experimental data can be reliably fitted by a linear function within the range from 25°C to 200°C (dashed blue curve). For larger temperatures, these should be extrapolated by using Eq. S1 (solid blue curve).

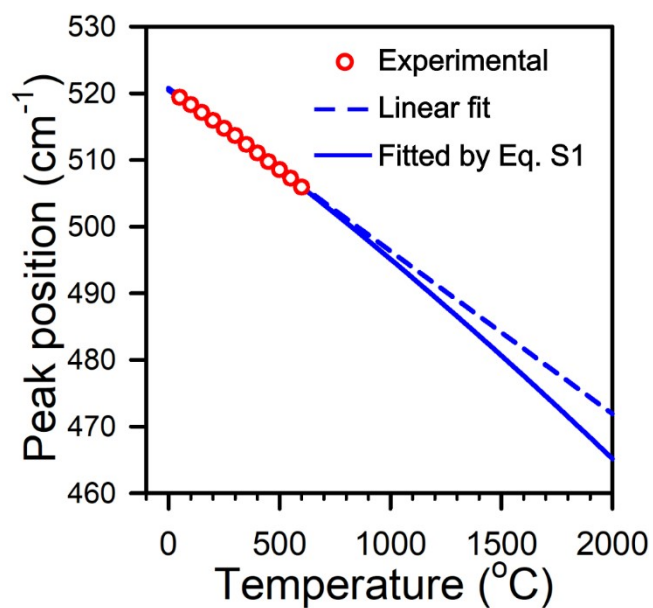


**Figure S2.** A plot of the peak position vs the temperature for pure silicon.

**An atomic force microscopy of a 2D array of TiN:Si voxels**

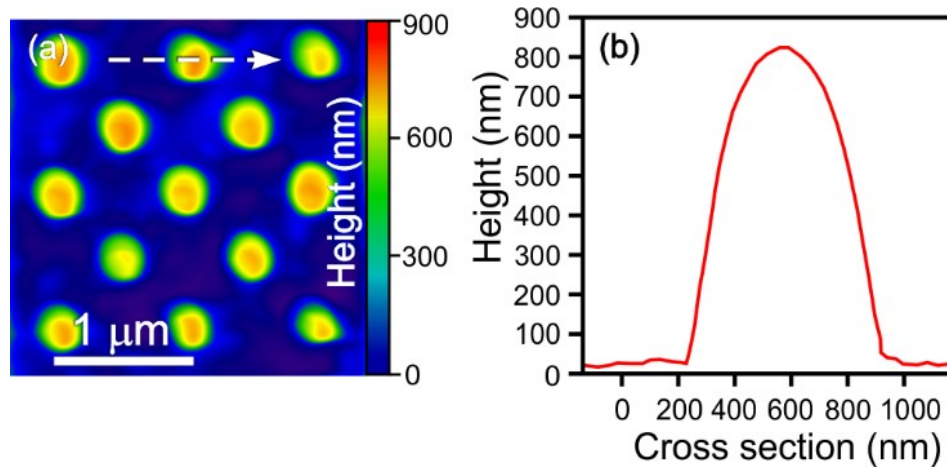


**Figure S3.** (a) AFM image of a 2D array of TiN:Si voxels shown in Fig. 2 (a2), and (b) its cross section along the dashed white arrow.

### A truncated square-shaped TiN:Si voxel

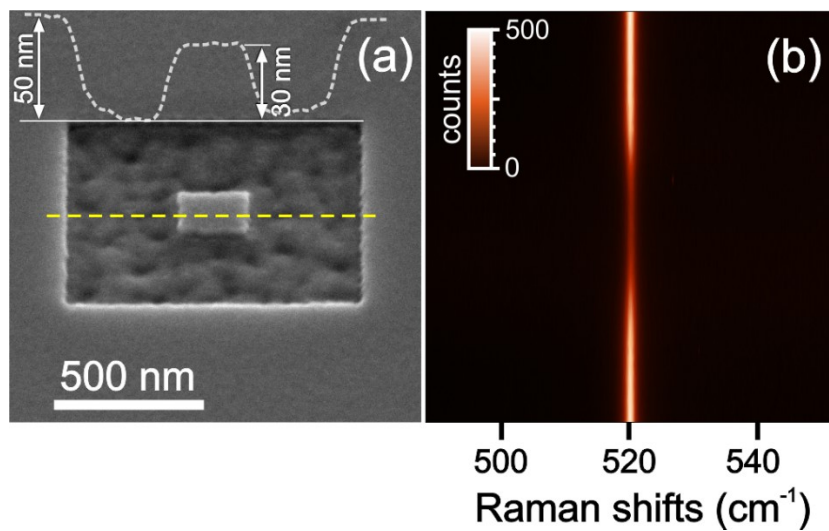


**Figure S4.** (a) A  $52^\circ$  tilted SEM image of the truncated square-shaped Si microstructure. The top inset shows an AFM cross section along the yellow dashed straight line. (b) a Raman waterfall of the microstructure along the yellow dashed straight line marked in Fig. S4 (a).

## Deconvolution of a composite Raman band

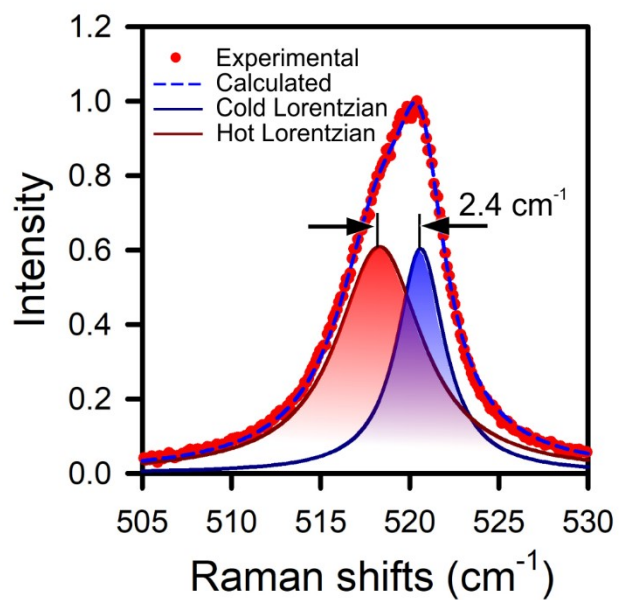


**Figure S5.** Deconvolution of a composite Raman band coming from a TiN:Si voxel into “hot” and “cold” Lorentzians.

### A temperature kinetics of a TiN:Si voxel under cw illumination

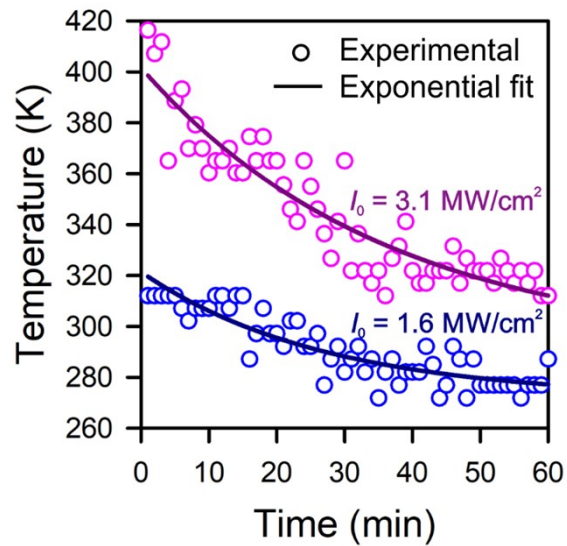


**Figure S6.** A temperature kinetics of a TiN:Si voxel under 633 nm laser illumination with different pump power.

## Light-induced oxidation of the central TiN:Si voxel

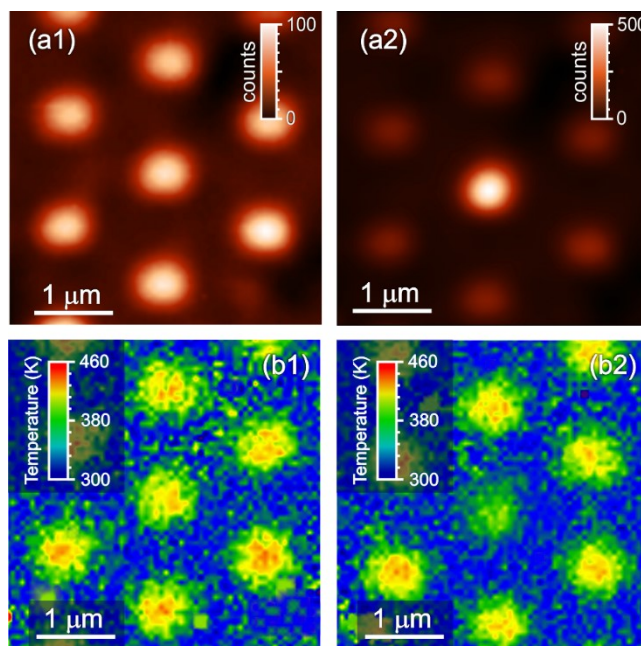


**Figure S7.** (a) Raman maps at 521 cm<sup>-1</sup> and (b) temperatures profiles before (1) and after (2) light-assisted annealing of the central TiN:Si voxel during 2 hours at the intensity of 5 MW/cm<sup>2</sup>.



## Light-induced oxidation of a 2D array of TiN:Si voxels

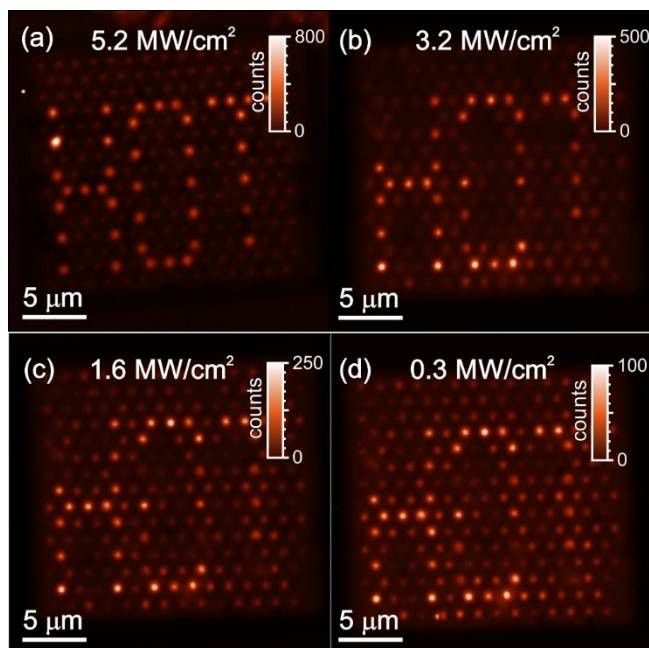


**Figure S8.** Raman maps of a 2D array of TiN:Si voxels with the engraved word “HOT” at different intensities.

1. H. Kang, G. H. Lee, H. Jung, J. W. Lee and Y. Nam, *ACS Nano*, 2018, **12**, 1128–1138.

### NOTES AND REFERENCES

1. K. Kneipp, H. Kneipp, *Faraday Discuss.*, 2006, **132**, 27–33.
2. K. Kneipp, Y. Wang, H. Kneipp, I. Itzkan, R.R. Dasari, M.S. Feld, *Phys. Rev. Lett.*, 1996, **76**(14), 2444–2447.
3. T.R. Hart, R.L. Aggarval, B. Lax, *Phys. Rev. B*, 1970, **1**(2), 638–642.
4. M. Balkanski, R.F. Wallis, E. Haro, *Phys. Rev. B*, 1983, **28**(4), 1928–1934.